Supporting Information

Synthesis, Characterization and Spectroscopic Investigation of Benzoxazole Conjugated Schiff Bases

Fabiano S. Santos,[a, b] Tania M. H. Costa,[a] Valter Stefani,[b] Paulo F. B. Gonçalves,[c] Rodrigo R. Descalzo,[c] Edilson V. Benvenutti[a,] and Fabiano S. Rodembusch[b,]**

Universidade Federal do Rio Grande do Sul

Instituto de Química

Avenida Bento Gonçalves, 9500. CP 15003. CEP 91501-970

Porto Alegre-RS, Brazil

Phone: +55 51 3308 7176. Fax: +55 51 3308 7304

[a]Laboratório de Sólidos e Superfícies, [b]Laboratório de Novos Materiais Orgânicos, [c]Grupo de Química Teórica e Computacional.

Emails: benvenutti@iq.ufrgs.br (E.V. Benvenutti); rodembusch@iq.ufrgs.br (F.S. Rodembusch)

SI 1. Spectroscopic characterization

SI 1.1. Precursors 3a-b

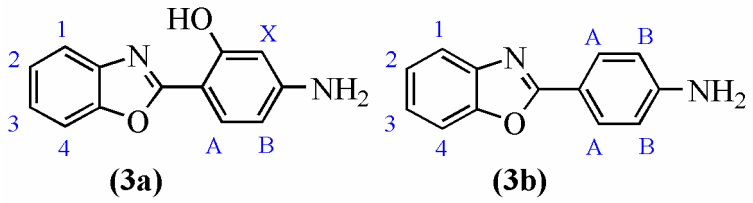

Figure SI 1. NMR attributions for the precursors **3a-b**.

Precursor 3a

Yield: 70%. IR (ATR, cm^{-1}): 3488 (ν_{asym} NH_2), 3382 (ν_{sym} NH_2), 3049 (ν_{arom} =CH), 1578 e 1556 (ν_{arom} C=C), 1620 (aromatic ring deformation). NMR-^{1}H (300 MHz, DMSO-d_6): δ (ppm) = 11.1 (s, 1H, OH), 7.70 (d, J_o = 8.6 Hz, 1H, H_A), 7.60 (m, 2H, H_1 and H_4), 7.30 (m, 2H, H_2 and H_3), 6.25 (dd, J_o = 8.6 Hz, J_m = 1.3 Hz, 1H, H_B), 6.00 (d, J_m = 1.3 Hz, 1H, H_X), 6.10 (s, 2H, NH_2).

Precursor 3b

Yield: 72%. IR (ATR, cm^{-1}): 3470 (ν_{asym} NH_2), 3294 (ν_{sym} NH_2), 3188 (Fermi's band), 3058 (ν_{arom} =CH), 1577 and 1558 (ν_{arom} C=C), 1602 (aromatic ring deformation). NMR-^{1}H (300 MHz, DMSO-d_6): δ (ppm) = 7.90 (d, J_o = 8.6 Hz, 2H, H_A), 7.63-7.68 (m, 2H, H_1 and H_4), 7.26-7.34 (m, 2H, H_2 and H_3), 6.74 (d, J_o = 8.6 Hz, 2H, H_B), 6.02 (s, 2H, NH_2).

SI 1.2. Attributions for NMR

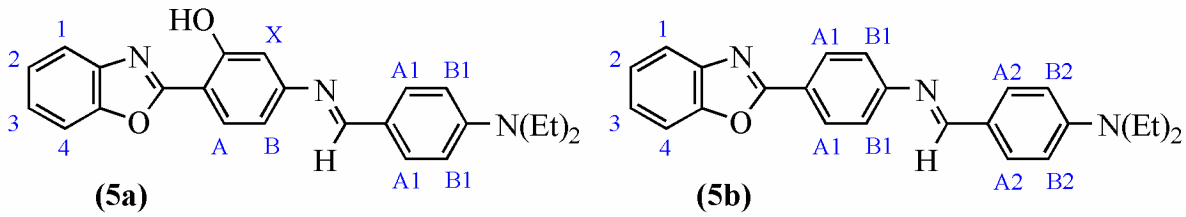

Figure SI 2. NMR attributions for the dyes **5a-b**.

SI 1.3. Original spectral data

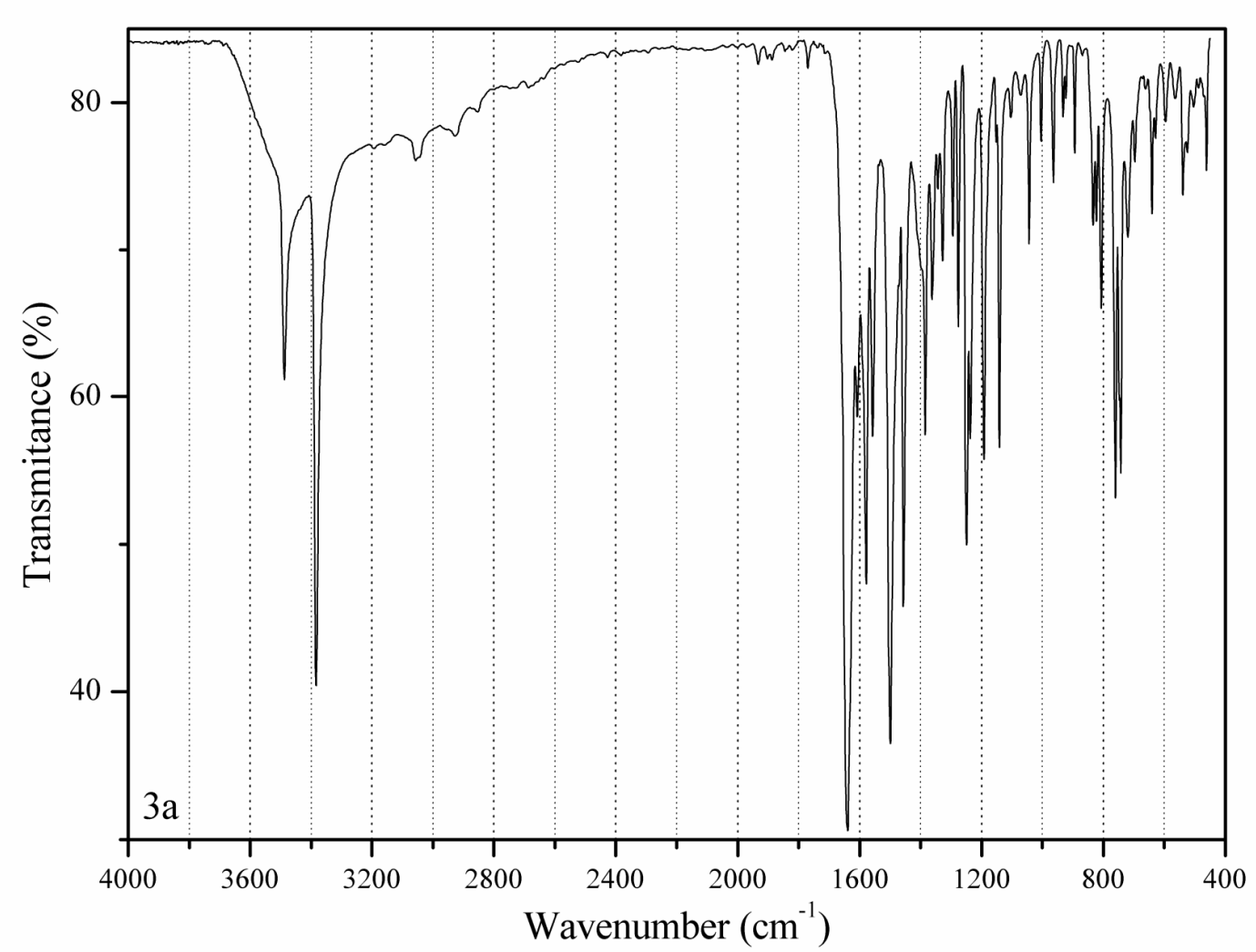

Figure SI 3. IR Absorption spectra (KBr) of the precursor **3a**.

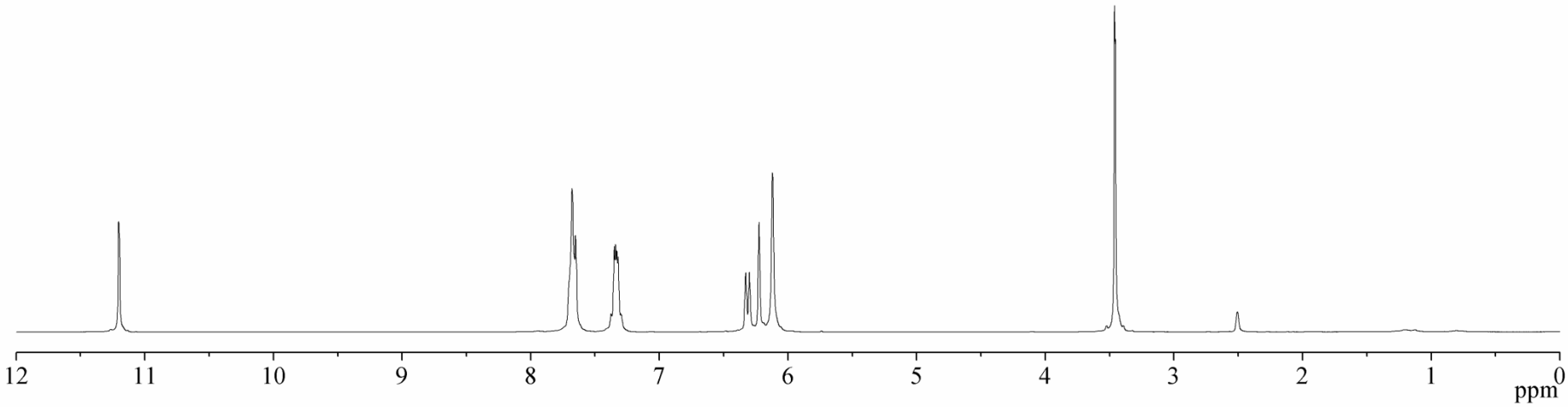

Figure SI 4. ^{1}H NMR (300 MHz, DMSO-d_6) spectra of the precursor **3a**.

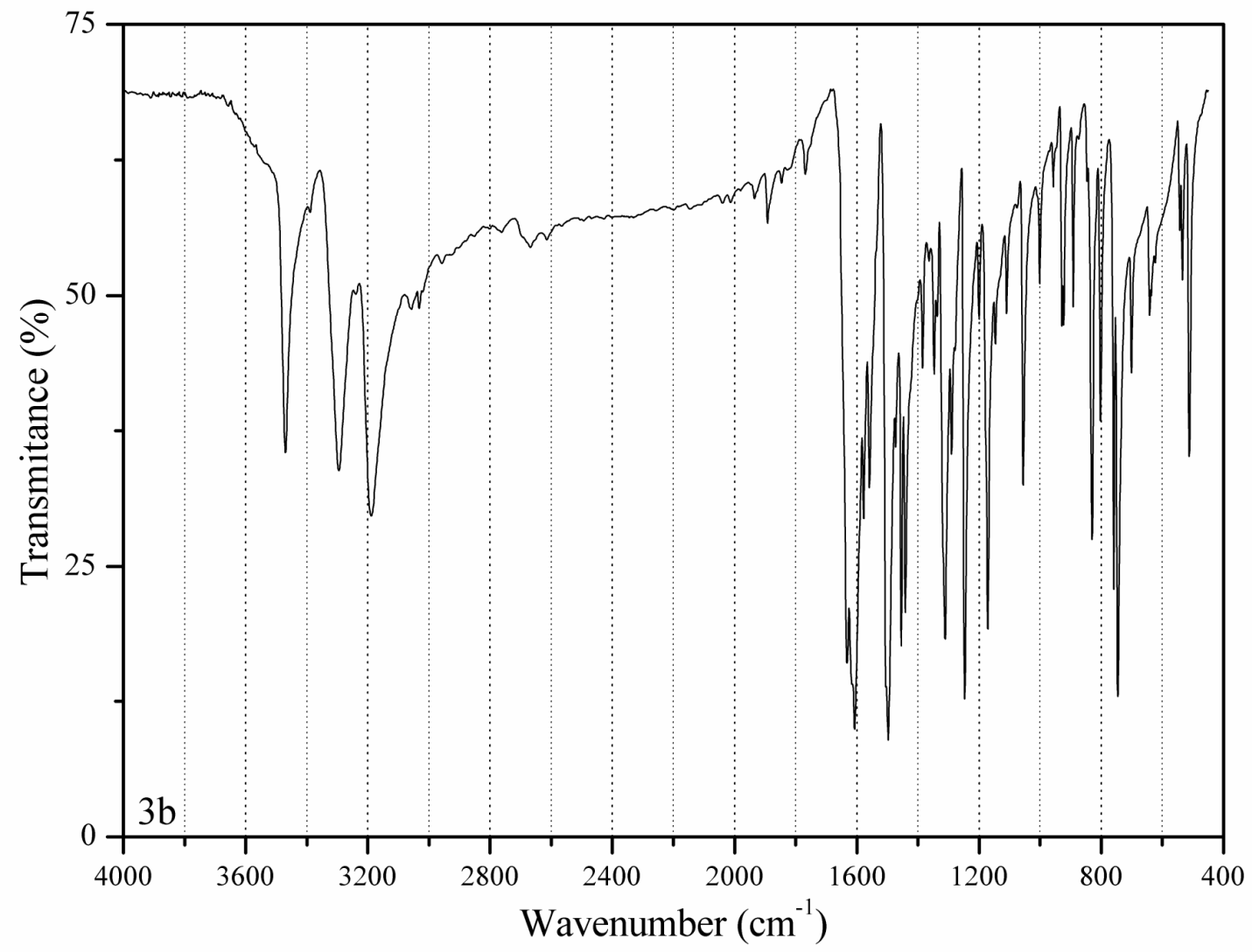

Figure SI 5. IR Absorption spectra (KBr) of the precursor **3b**.

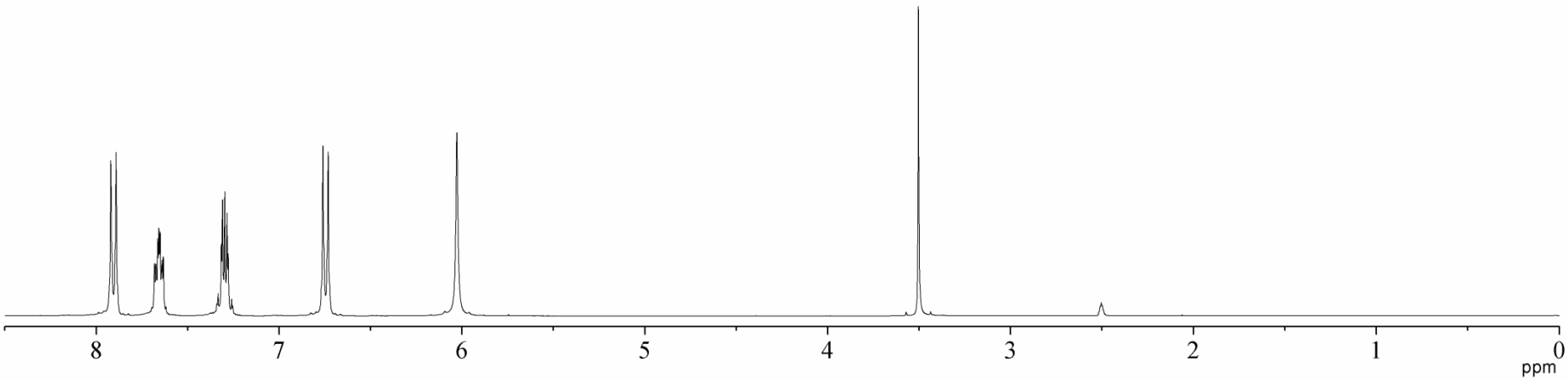

Figure SI 6. ^{1}H NMR (300 MHz, DMSO-d_6) spectra of the precursor **3b**.

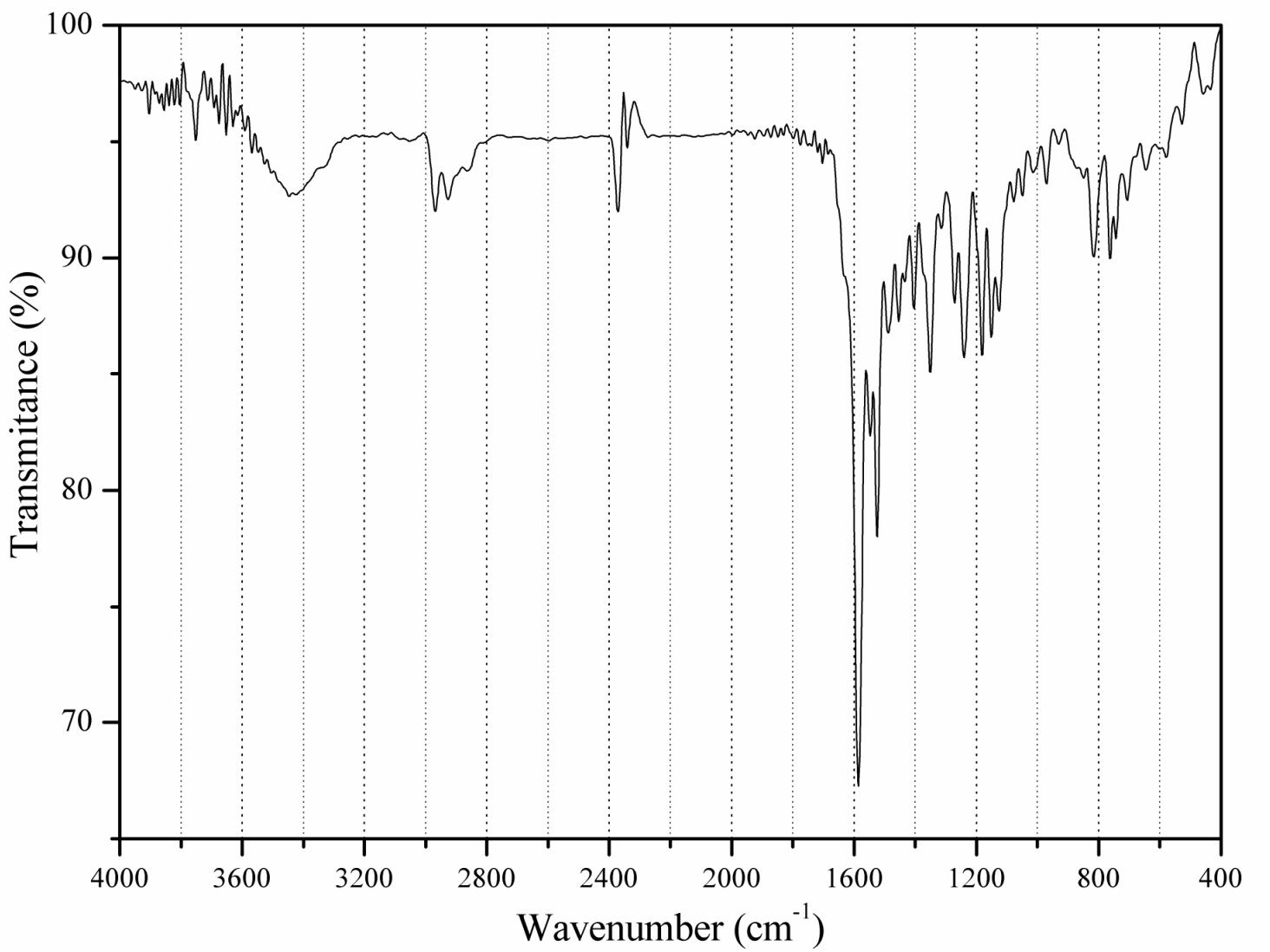

Figure SI 7. IR Absorption spectra (ATR) of the dye **5a**.

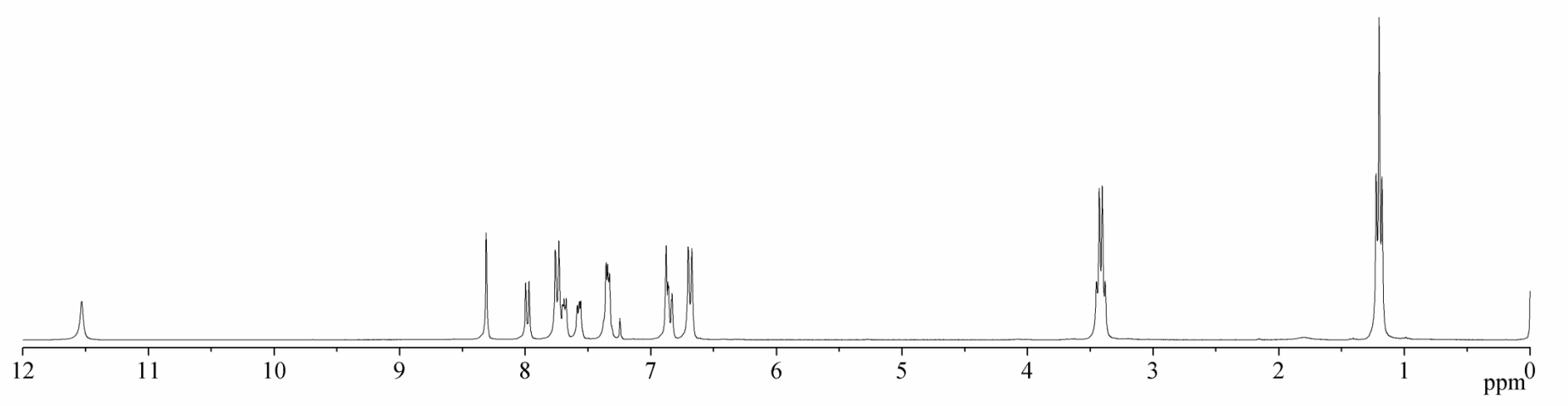

Figure SI 8. ^{1}H NMR (300 MHz, $CDCl_3$) spectra of the dye **5a**.

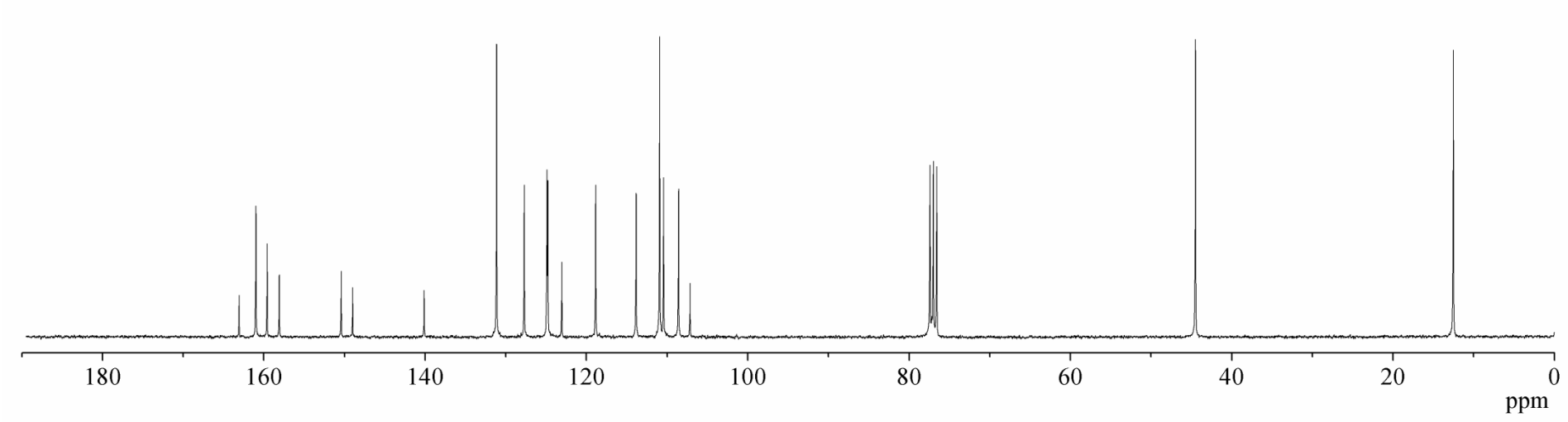

Figure SI 9. ^{13}C NMR (75,4 MHz, $CDCl_3$) spectra of the dye **5a**.

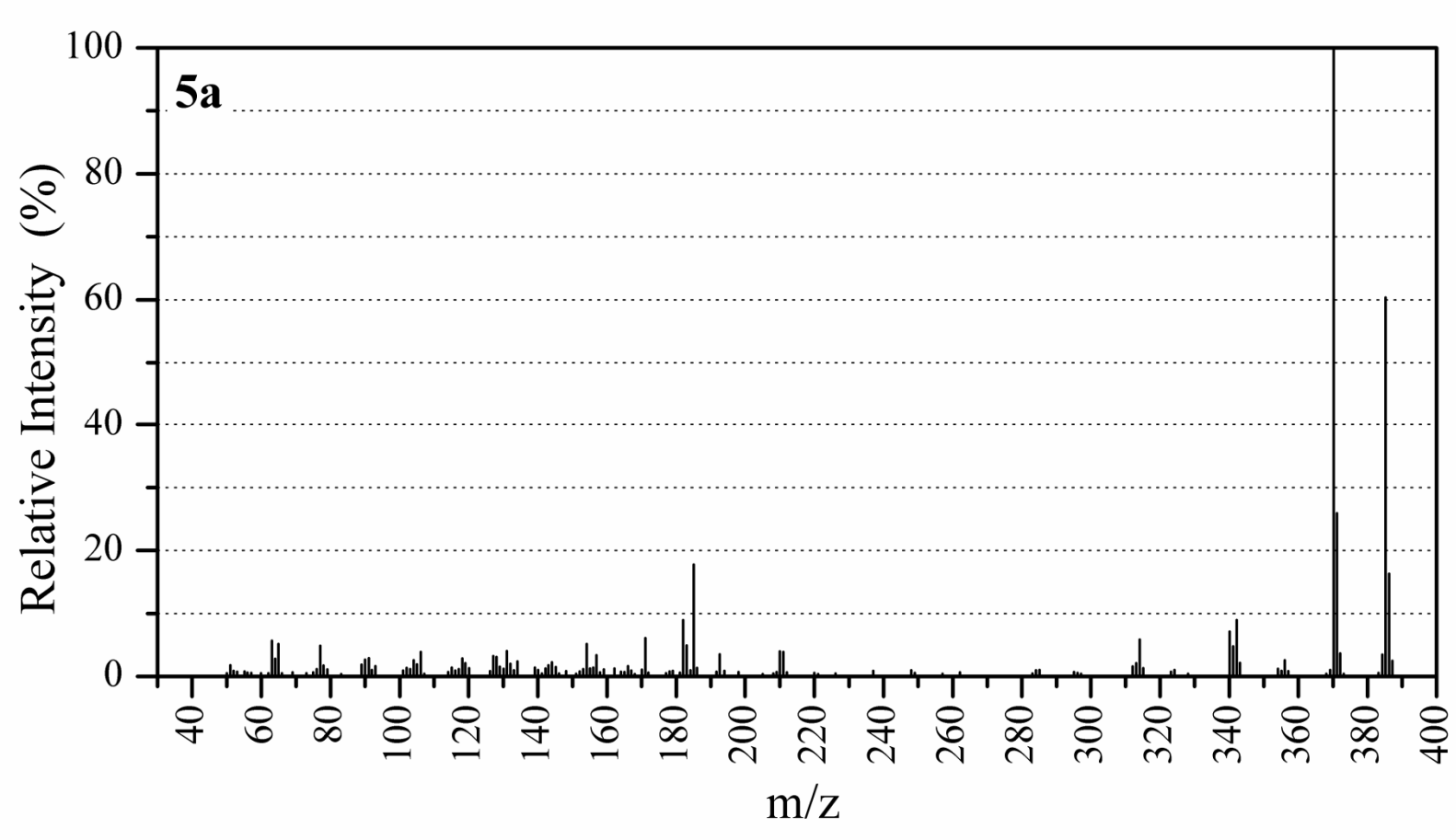

Figure SI 10. EIMS fragmentation pattern of the dye **5a**.

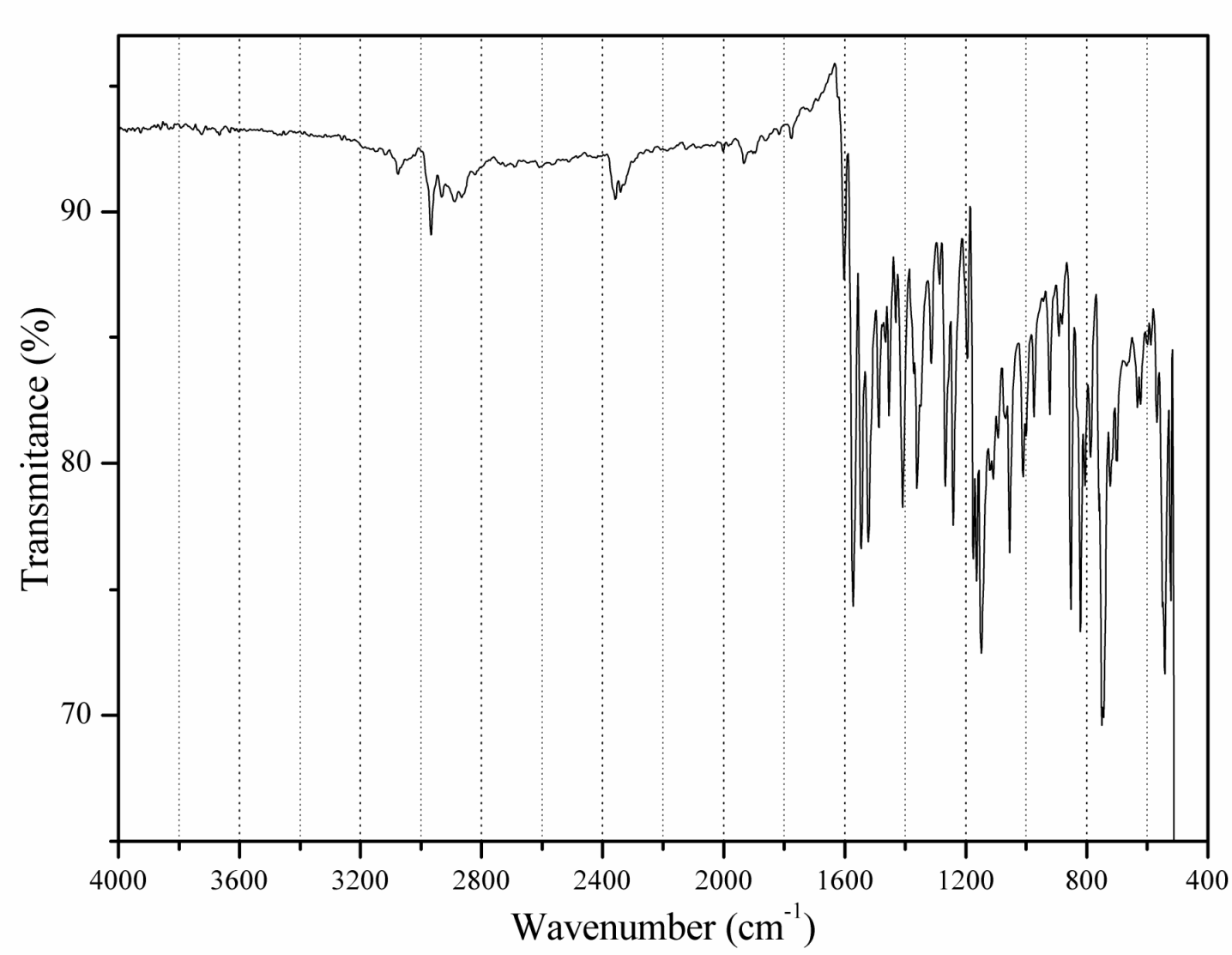

Figure SI 11. IR Absorption spectra (ATR) of the dye **5b**.

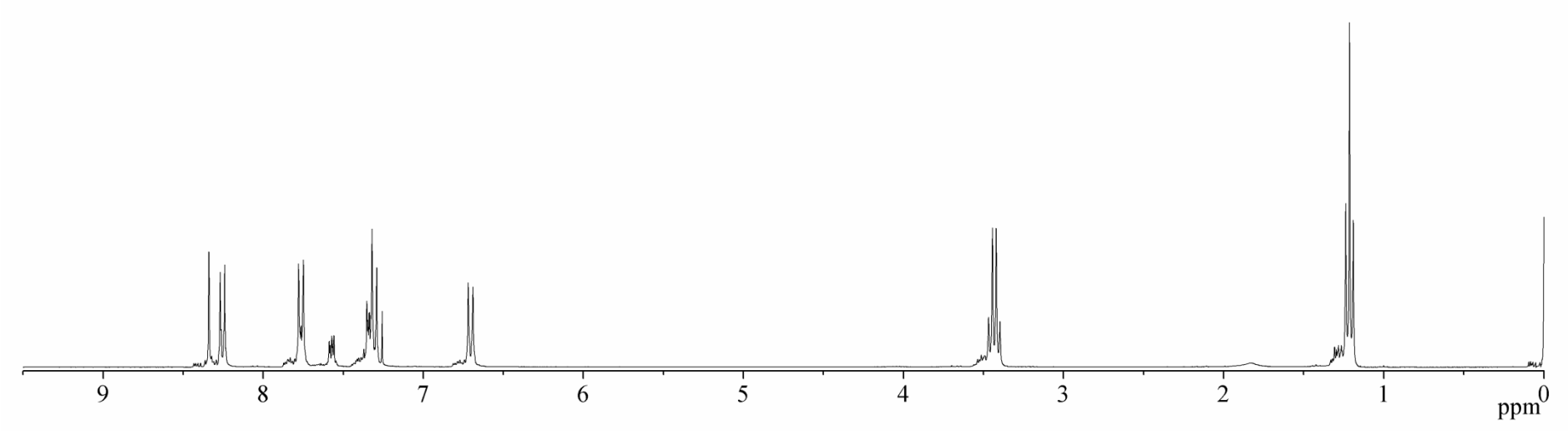

Figure SI 12. ^{1}H NMR (300 MHz, $CDCl_3$) spectra of the dye **5b**.

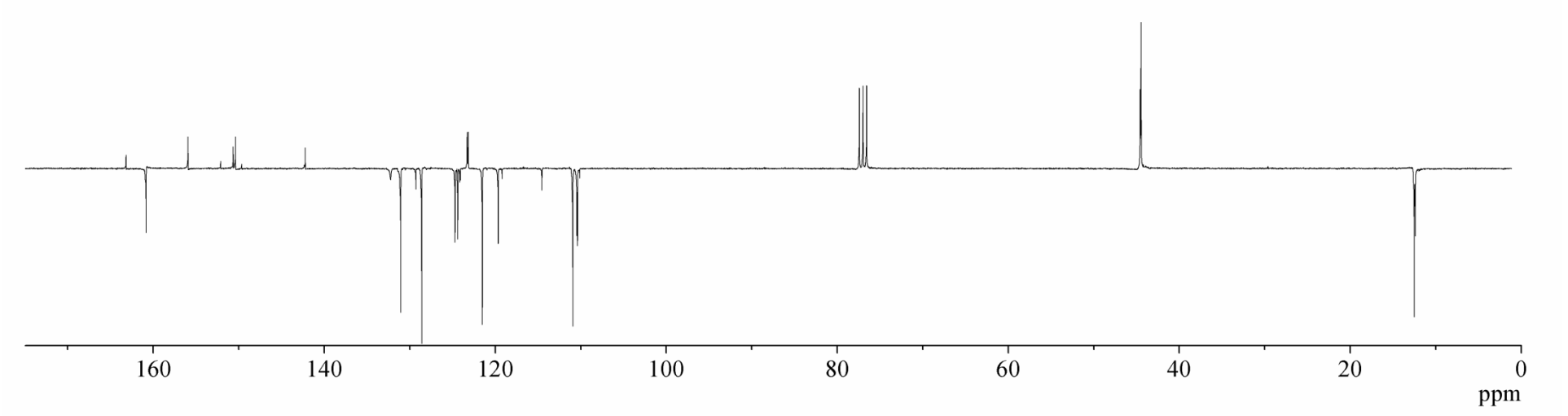

Figure SI 13. APT (75,4 MHz, $CDCl_3$) spectra of the dye **5b**.

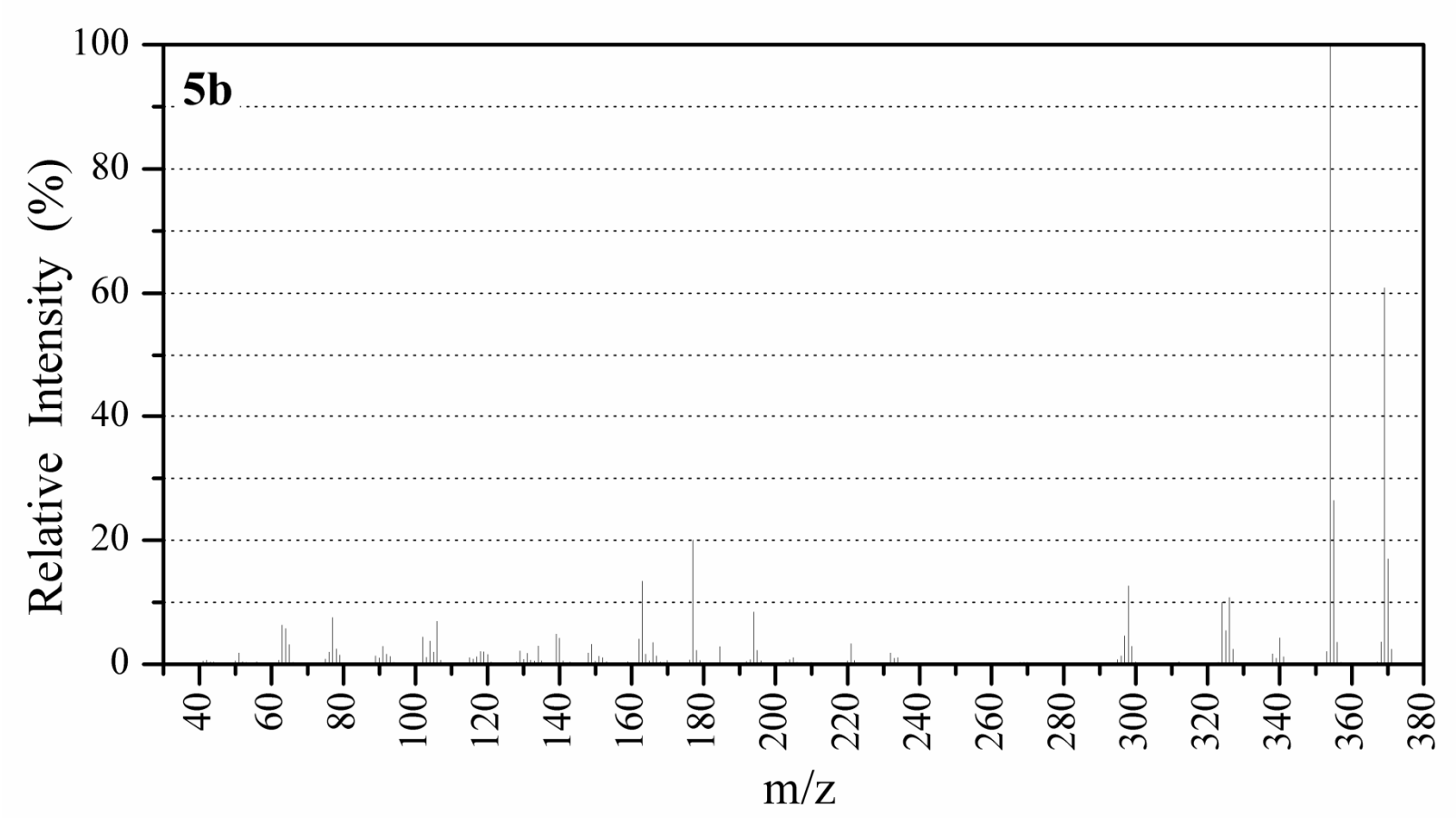

Figure SI 14. EIMS fragmentation pattern of the dye **5b**.

SI 2. Photophysical Data

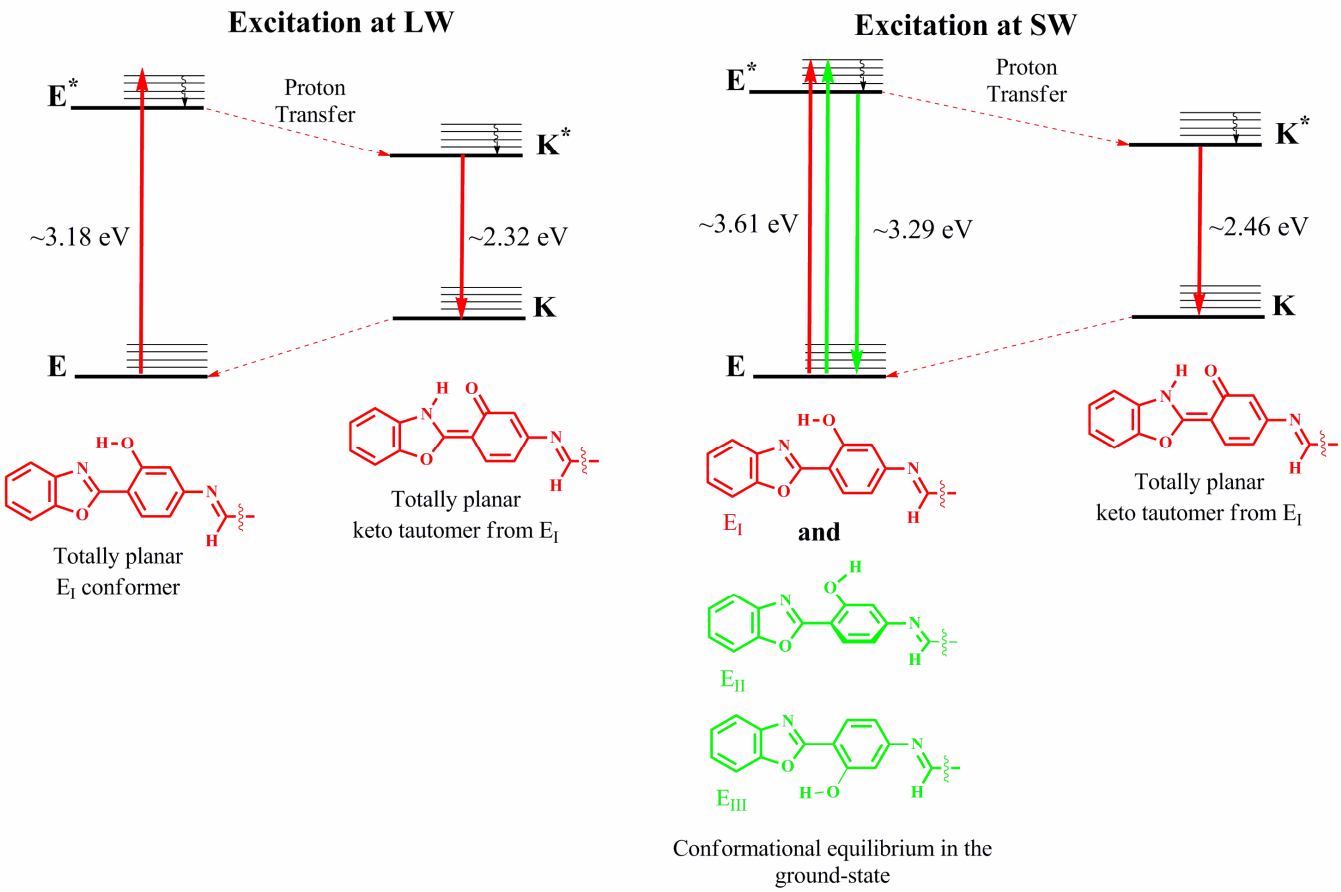

Figure SI 15. General Scheme of the ESIPT mechanism in the dye **5a**. The absorption and emission values are from the photophysical data (see Table 1 and 2 in the manuscript).

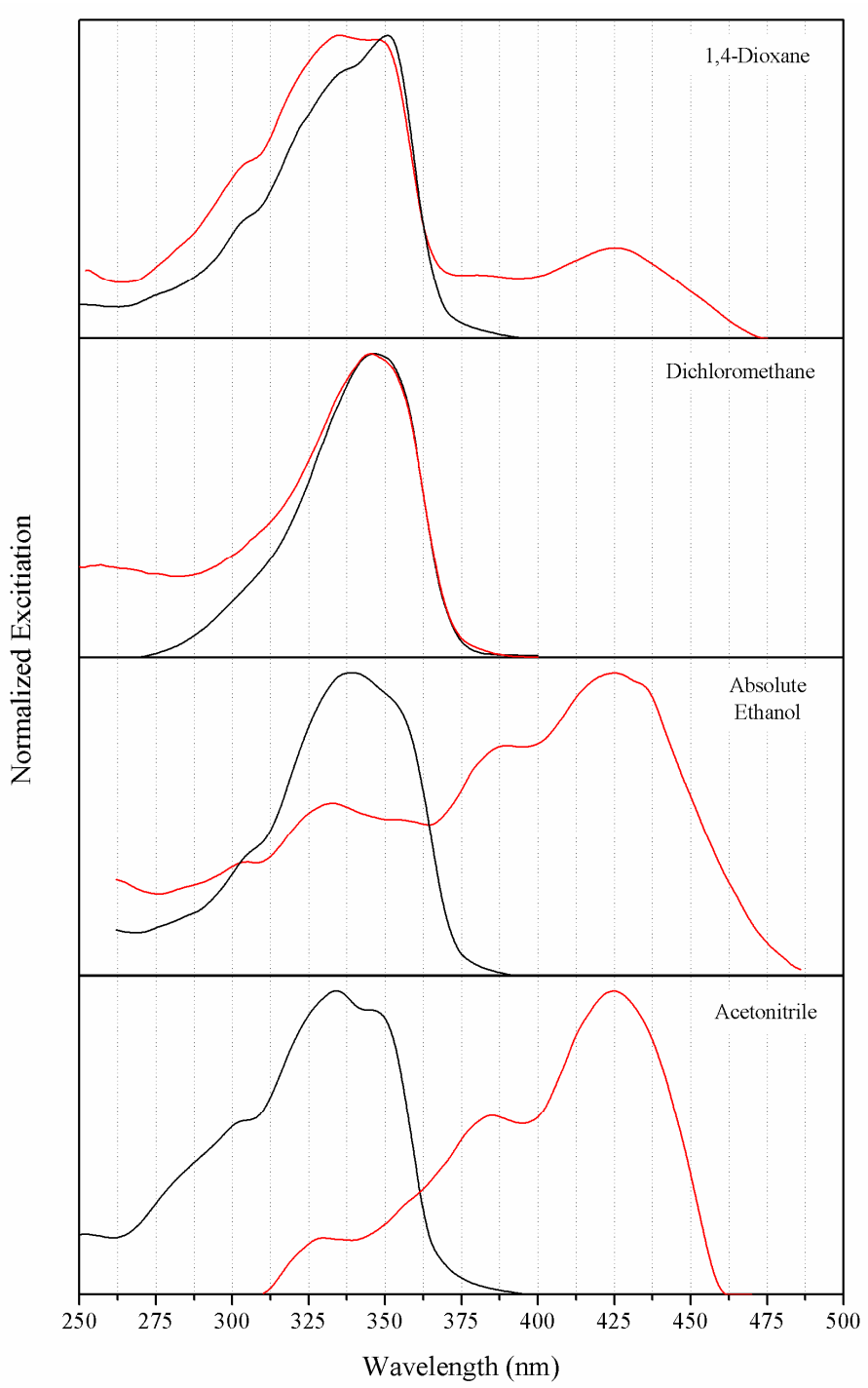

Figure SI 16. Normalized Excitation spectra of the dye **5a** using the normal emission (black solid line) and the keto emission (red solid line) as observation wavelengths.

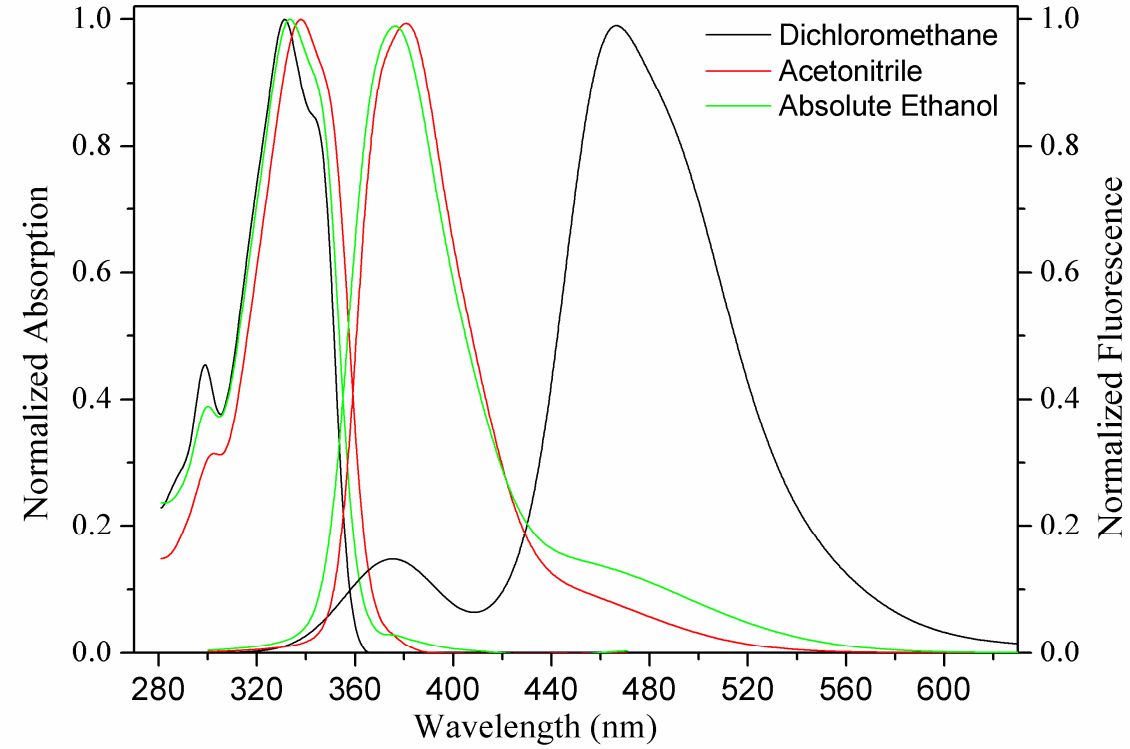

Figure SI 17. Normalized UV-Vis absorption and fluorescence emission of **3a**.

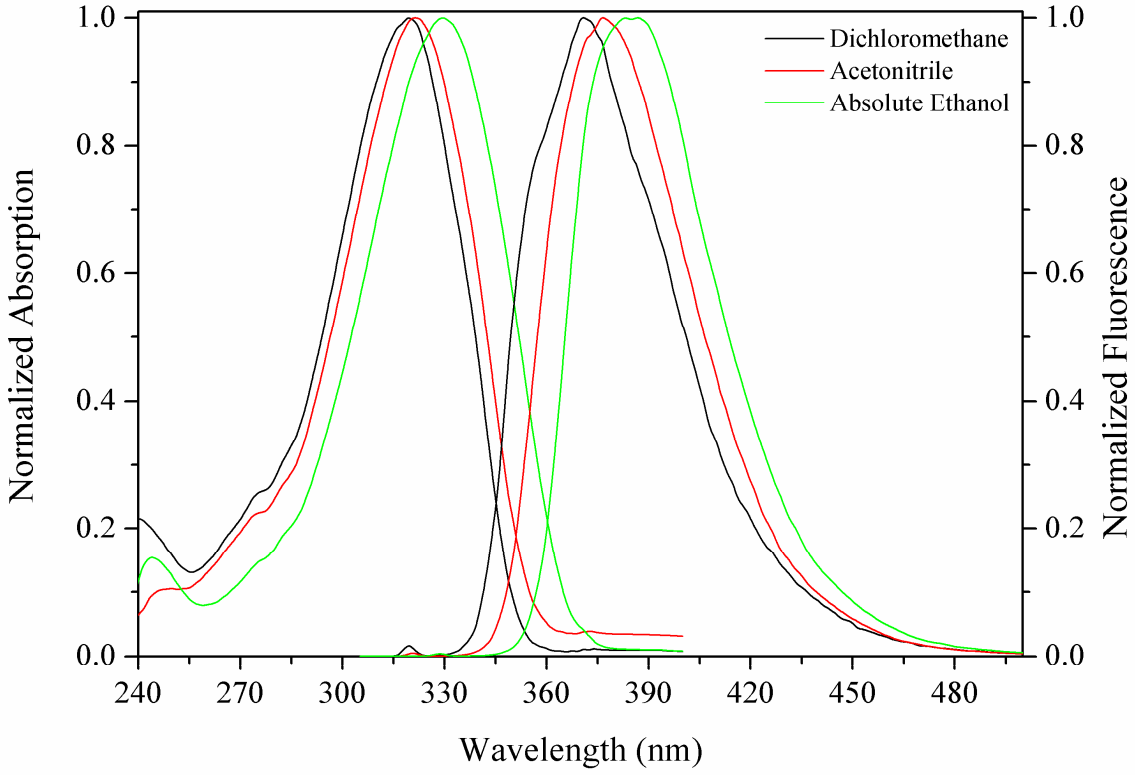

Figure SI 18. Normalized UV-Vis absorption and fluorescence emission of **3b**.

Table SI1. Spectroscopic data from precursor **3a**.

Solvent	λ_{abs} (nm)	ε (x 10^4) (M^{-1} cm^{-1})	λ_{em} (nm)	$\Delta\lambda_{ST}$ (nm)	Φ_{fl}*	[ ] (mol/L)
CH_2Cl_2	332	2.8	467	135	0.012	1.6×10^{-5}
CH_3CN	334	1.5	378	42	0.023	3.2×10^{-5}
EtOH	335	5.3	376	43	0.025	2.6×10^{-5}

Table SI2. Spectroscopic data from precursor **3b**.

Solvent	λ_{abs} (nm)	ε (x 10^4) (M^{-1} cm^{-1})	λ_{em} (nm)	$\Delta\lambda_{ST}$ (nm)	Φ_{fl}*	[ ] (mol/L)
CH_2Cl_2	319	3.00	371	52	0.58	2.1×10^{-5}
CH_3CN	321	3.13	376	55	0.51	2.3×10^{-5}
EtOH	330	0.35	385	55	0.48	1.22×10^{-4}

* Using quinine sulphate as fluorescence quantum yield standard.

SI 3. Theoretical information data

SI 3.1. Dye 5a

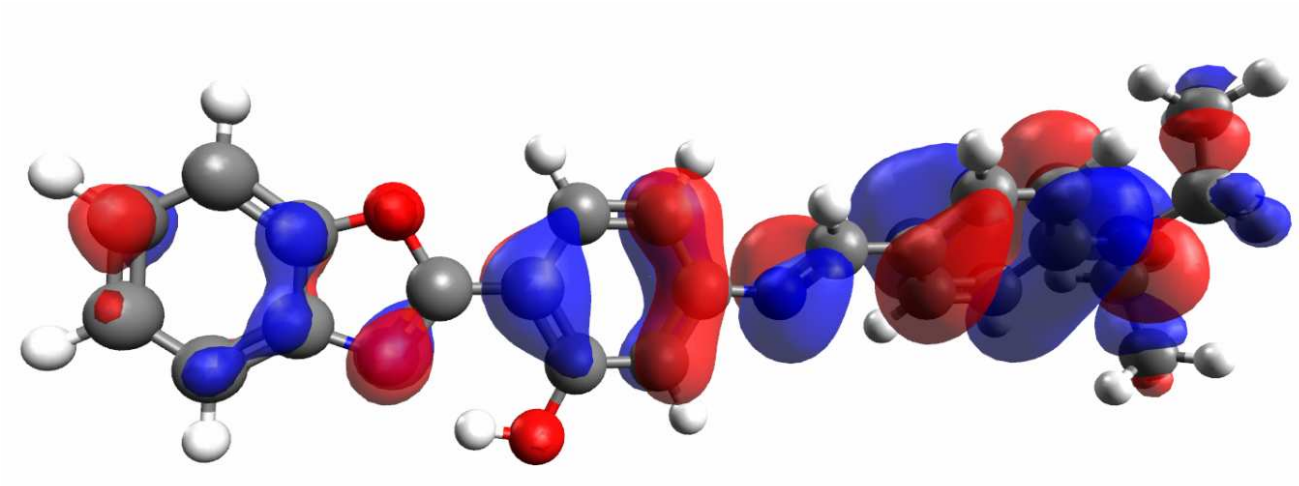

Figure SI 19. Superior view of the HOMO orbitals for **5a.**

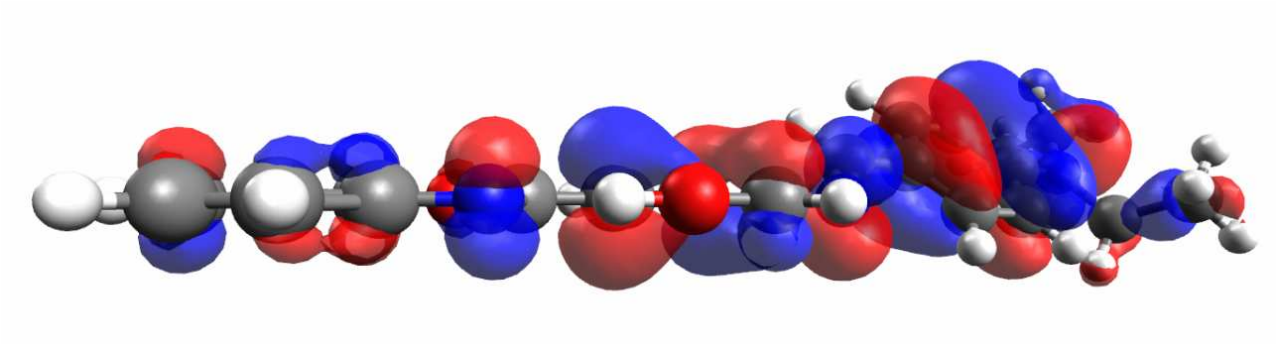

Figure SI 20. Lateral view of the HOMO orbitals for **5a.**

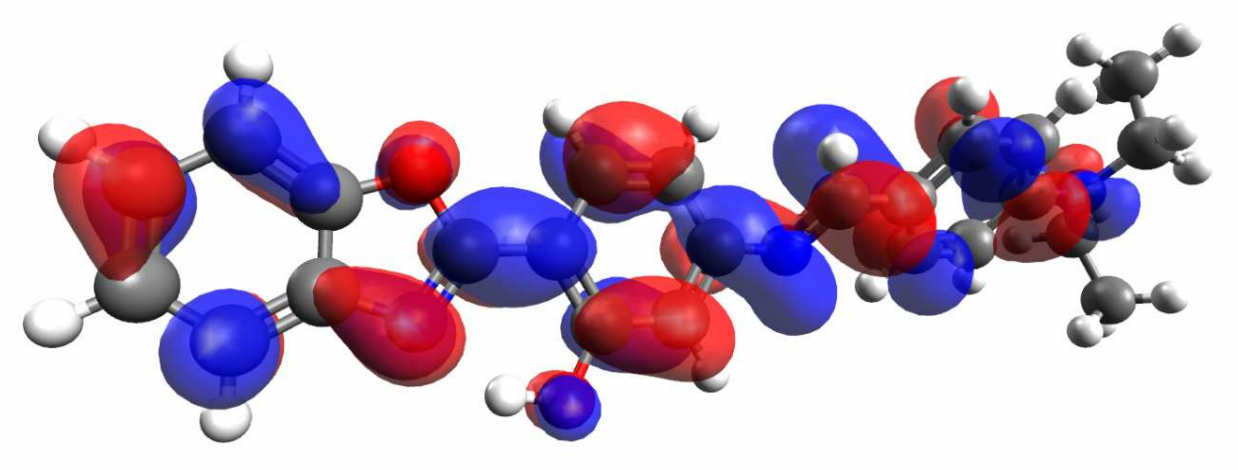

Figure SI 21. Superior view of the LUMO orbitals for **5a.**

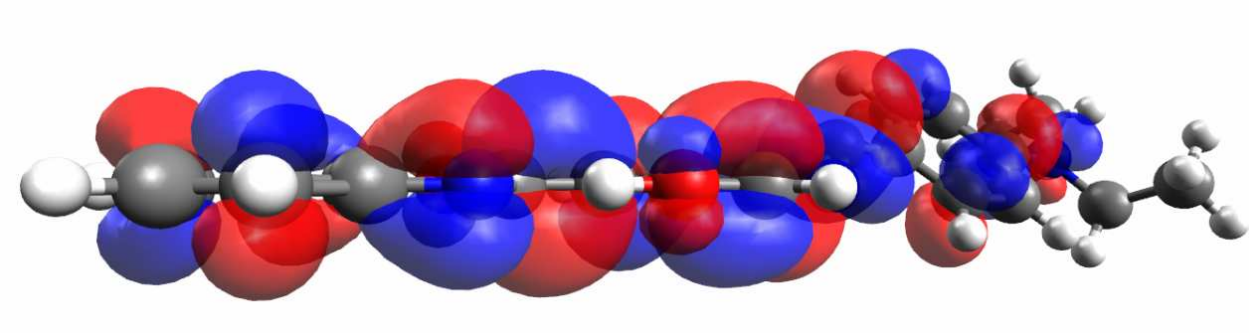

Figure SI 22. Lateral view of the LUMO orbitals for **5a.**

SI 3.2. Dye 5b

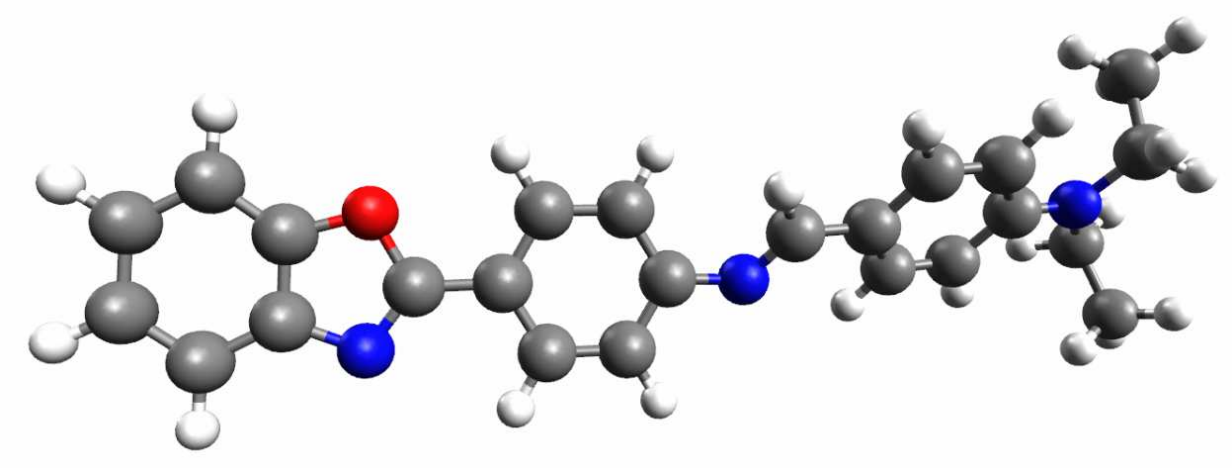

Figure SI 23. Structure of the Schiff base **5b** in the ground state.

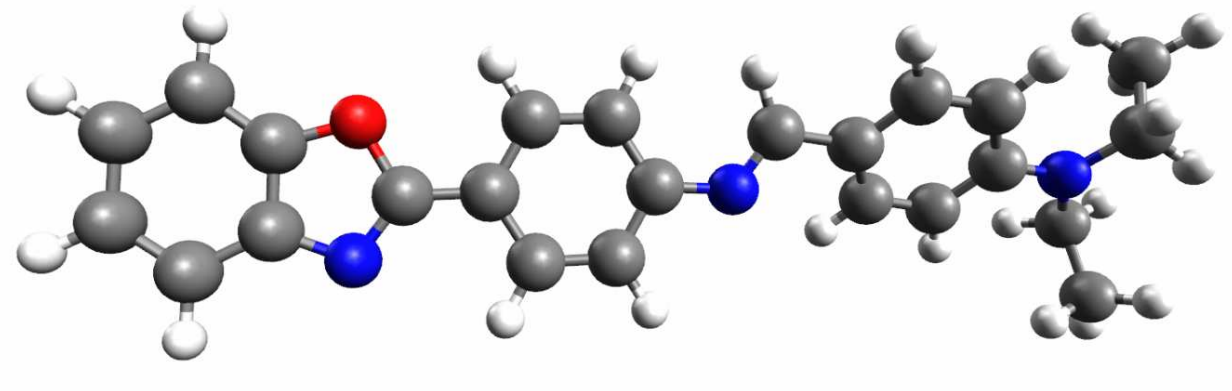

Figure SI 24. Structure of the Schiff base **5b** in the excited state.

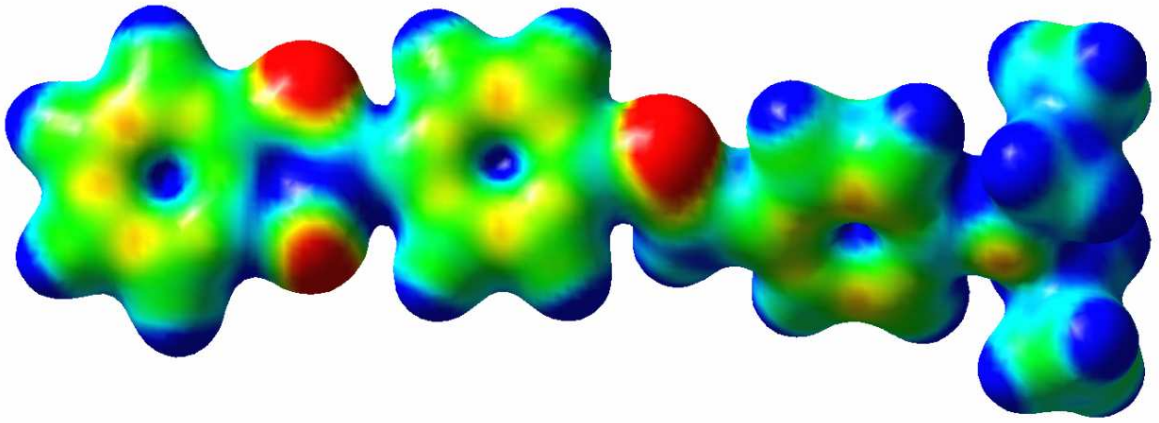

Figure SI 25. Electrostatic potential surfaces of the Schiff base **5b** in the ground state.

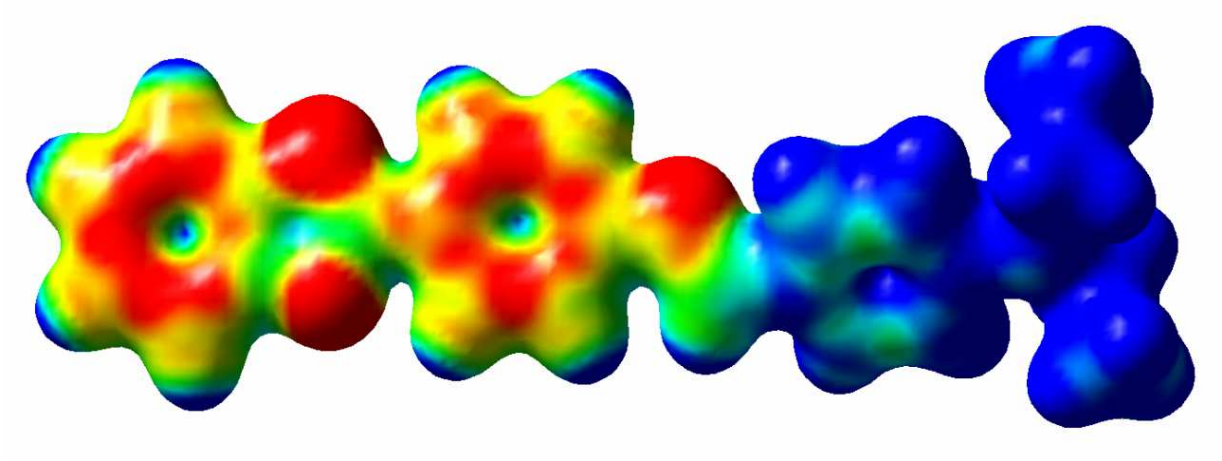

Figure SI 26. Electrostatic potential surfaces of the Schiff base **5b** in the excited state.

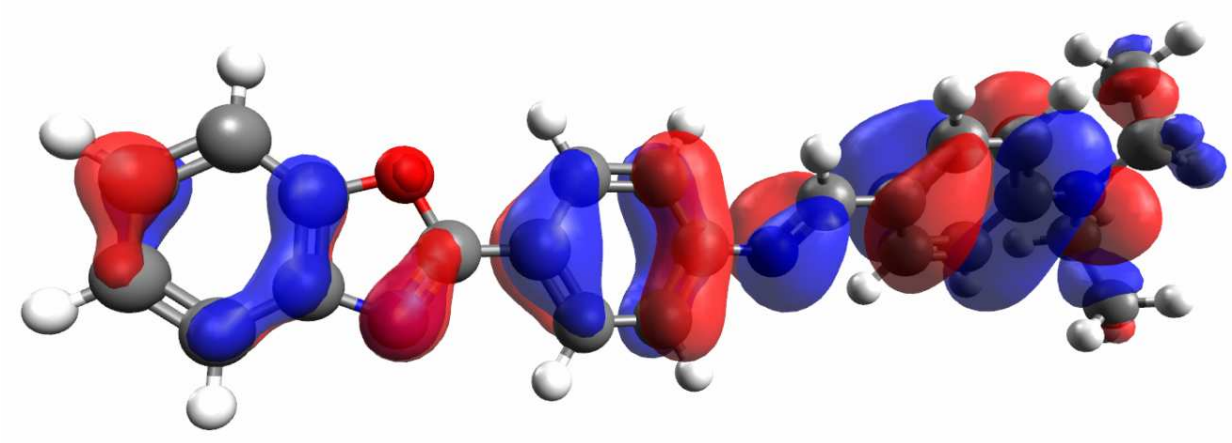

Figure SI 27. Superior view of the HOMO orbitals for **5b**.

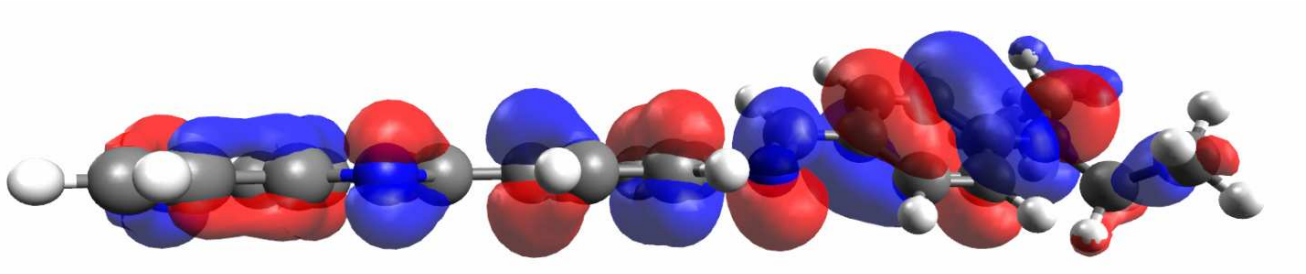

Figure SI 28. Lateral view of the HOMO orbitals for **5b**.

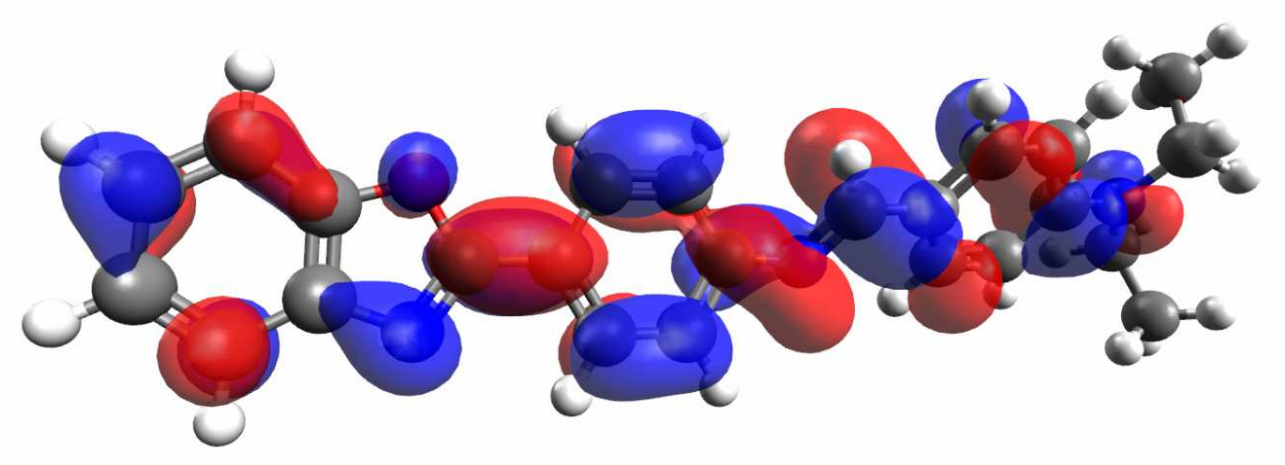

Figure SI 29. Superior view of the LUMO orbitals for **5b**.

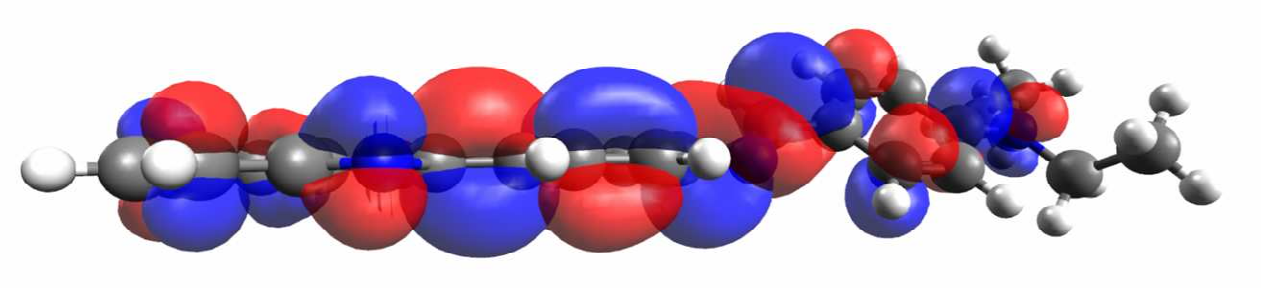

Figure SI 30. Lateral view of the LUMO orbitals for **5b**.